Nanoscale

PAPER

View Article Online
View Journal | View Issue

Cite this: *Nanoscale*, 2019, **11**, 11159

Chirality enriched carbon nanotubes with tunable wrapping *via* corona phase exchange purification (CPEP)†

Robert Nißler, Florian A. Mann, Helen Preiß, Gabriele Selvaggio, Niklas Herrmann and Sebastian Kruss *

Single-walled carbon nanotubes (SWCNTs) have unique photophysical properties and serve as building blocks for biosensors, functional materials and devices. For many applications it is crucial to use chirality-pure SWCNTs, which requires sophisticated processes. Purification procedures such as wrapping by certain polymers, phase separation, density gradient centrifugation or gel chromatography have been developed and yield distinct SWCNT species wrapped by a specific polymer or surfactant. However, many applications require a different organic functionalization (corona) around the SWCNTs instead of the one used for the purification process. Here, we present a novel efficient and straightforward process to gain chirality pure SWCNTs with tunable functionalization. Our approach uses polyfluorene (PFO) polymers to enrich certain chiralities but the polymer is removed again and finally exchanged to any desired organic phase. We demonstrate this concept by dispersing SWCNTs in poly[(9,9-dioctylfluorenyl-2,7-diyl)-*alt*-*co*-(6,6′-{2,2′-bipyridine})] (PFO-BPy), which is known to preferentially solubilize (6,5)-SWCNTs. Then PFO-BPy is removed and recycled, while letting the SWCNTs adsorb/agglomerate on sodium chloride (NaCl) crystals, which act as a toluene-stable but water-soluble filler material. In the last step these purified SWCNTs are redispersed in different polymers, surfactants and ssDNA. This corona phase exchange purification (CPEP) approach was also extended to other PFO variants to enrich and functionalize (7,5)-SWCNTs. CPEP purified and functionalized SWCNTs display monodisperse nIR spectra, which are important for fundamental studies and applications that rely on spectral changes. We show this advantage for SWCNT-based nIR fluorescent sensors for the neurotransmitter dopamine and red-shifted sp^3 defect peaks (E_{11}^*). In summary, CPEP makes use of PFO polymers for chirality enrichment but provides access to chirality enriched SWCNTs functionalized in any desired polymer, surfactant or biopolymer.

Received 16th April 2019,
Accepted 25th May 2019

DOI: 10.1039/c9nr03258d

rsc.li/nanoscale

Introduction

One of the great challenges in nanoscience is to obtain materials of well-defined structure and size.[1,2] Polydisperse nanomaterials can lead to wrong conclusions in fundamental studies on structure–function relationships but also affect performance in applications. Therefore, progress in synthesis and purification of nanomaterials is crucial to advance the whole nanotechnology field. An important class of nanomaterials are single walled carbon nanotubes (SWCNTs).[3,4] Semiconducting SWCNTs are fluorescent in the near infrared (nIR) region and the emission wavelength depends on their structure described by the chirality or chiral index (*n*,*m*).[5–9] The nIR fluorescence of SWCNTs has been used for example for imaging, biosensing or single-photon generation.[10–14] Even though the synthesis of specific SWCNT chiralities has seen progress over the past years typical SWCNT starting materials still contain multiple chiralities.[15–17] Therefore, purification and separation of SWCNTs remains a major area of research.

Different approaches have been developed that separate SWCNTs according to length, diameter and chirality.[18–22] The most used purification protocols are based on density gradient centrifugation,[23,24] phase separation,[25–27] gel chromatography[28–31] or ion exchange chromatography.[32] In most of these approaches surfactants such as sodium dodecyl sulfate (SDS) or sodium cholate (SC) are used to disperse SWCNTs in aqueous solution. Other methods rely on the favored interaction of specific macromolecules/polymers with a certain SWCNT chirality. A very powerful approach is based on certain ssDNA sequences that disperse specific chiralities.[33,34] In organic solvents polymers of the polyfluor-

Institute of Physical Chemistry, Göttingen University, Germany.
E-mail: skruss@uni-goettingen.de

†Electronic supplementary information (ESI) available. See DOI: 10.1039/c9nr03258d

ene (PFO) family such as poly[(9,9-dioctylfluorenyl-2,7-diyl)-*alt*-*co*-(6,6′-{2,2′-bipyridine})] (PFO-PBy) have been used to enrich for example (6,5)-SWCNTs.[35–38] Most of the purification methods yield chirality-enriched SWCNTs with fixed organic phase (corona) compositions, either in non-biocompatible surfactants/polymers or with fixed ssDNA sequences. Especially for biosensing applications water-dispersable SWCNTs are required and specific surface modifications are crucial to tailor molecular interactions.[11,14,39] It was shown that the sequence of ssDNA modified SWCNTs has a dramatic impact on colloidal properties and the nIR-fluorescence response/kinetics to analytes.[40–43] For example, $(GT)_{10}$ – ssDNA functionalized SWCNTs report secretion of the neurotransmitter dopamine and can even discriminate between different catecholamines.[44,45] Many other non-covalent functionalization concepts with DNA/peptide hybrids, xeno nucleic acids, peptide barrels, sugars, lipids and antibodies have been developed to tailor SWCNT properties.[46–52] Most of these approaches would profit from a general access to chirality enriched SWCNTs instead of the polydisperse SWCNT starting material that is typically used. Isolation procedures of distinct SWCNT chiralities and further corona phase modification to other ssDNA sequences, phospholipids or surfactants have only been reported in a few specific cases.[53–56] In principle it is therefore possible to remove surfactants from enriched SWCNTs, as shown for distinct PFO-SWCNTs,[57–61] but a general procedure is still missing. One challenge is to avoid strong aggregation of purified SWCNTs during the process, which could hamper redispersion.

Here, we report a general but straightforward route to chirality enriched SWCNTs with tunable wrapping. We make use of the high-selectivity of PFO polymers for certain chiralities, remove/recycle the PFO polymer and obtain a chirality enriched SWCNT material stabilized in a NaCl filler/scaffold to avoid strong aggregation. This material is then used for different non-covalent functionalization approaches and the advantages of monodisperse SWCNTs are shown for different applications.

Results and discussion

To get access to nearly chirality-pure SWCNTs with any desired non-covalent functionalization we developed a three-step approach.

It makes use of the high selectivity of polymers of the PFO family for certain SWCNT chiralities. Then the PFO-polymer is removed and recycled, while the purified SWCNTs can be further surface modified *via* standard tip sonication. This corona phase exchange purification (CPEP) approach makes the organic phase independent of the surfactant and polymer used for purification, which is crucial for most applications of SWCNTs.

The CPEP approach (see Fig. 1) is based on the high selectivity of PFO-BPy for (6,5)-SWCNTs. A CoMoCAT SWCNT sample is dispersed with PFO-BPy in toluene *via* shear force mixing and separated from larger bundles by centrifugation.[36] The highly enriched PFO-BPy-(6,5)-SWCNTs are precipitated with isopropyl alcohol (4 : 1, toluene : isopropyl alcohol), while the excess PFO-polymer stays in solution after centrifugation (Fig. 2a). Redispersion of the SWCNT pellet in toluene and repeated precipitation decreased the concentration of the free PFO-BPy to a minimum, which can be monitored by UV-Vis-nIR absorbance spectroscopy (Fig. 2a). The purified nanotubes were then transferred to a solvent-resistant filter loaded with NaCl crystals, which act as toluene-resistant, but later on water-soluble filler/scaffold (see ESI Fig. S1†). Washing with hot toluene removed the remaining PFO-BPy from the (6,5)-

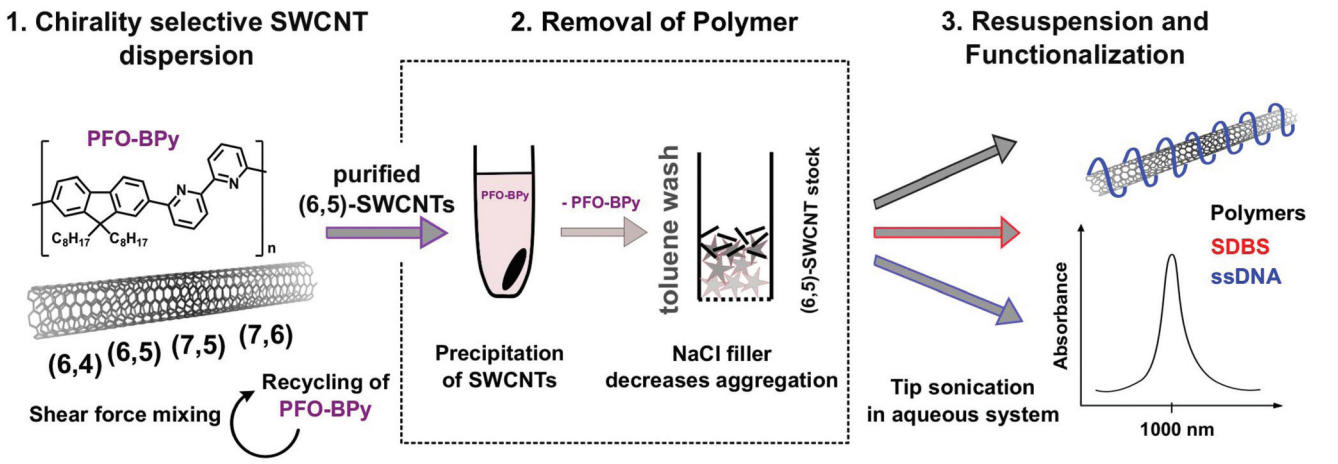

Fig. 1 Schematic of the corona phase exchange purification (CPEP) process. The process is based on selective dispersion of (6,5)-SWCNTs by PFO-BPy or certain SWCNT chiralities by other members of the PFO family in toluene. PFO-BPy is removed by adding isopropyl alcohol, which precipitates the SWCNTs, while the majority of PFO-BPy stays in solution and can be recycled. The (6,5)-SWCNT pellet is transferred to a solvent-resistant filter equipped with NaCl crystals, which act as water-soluble filler material during removal of remaining PFO-BPy residues. The (6,5)-SWCNT flakes are then available for any functionalization approach *e.g.* with ssDNA, SDBS or biopolymers.

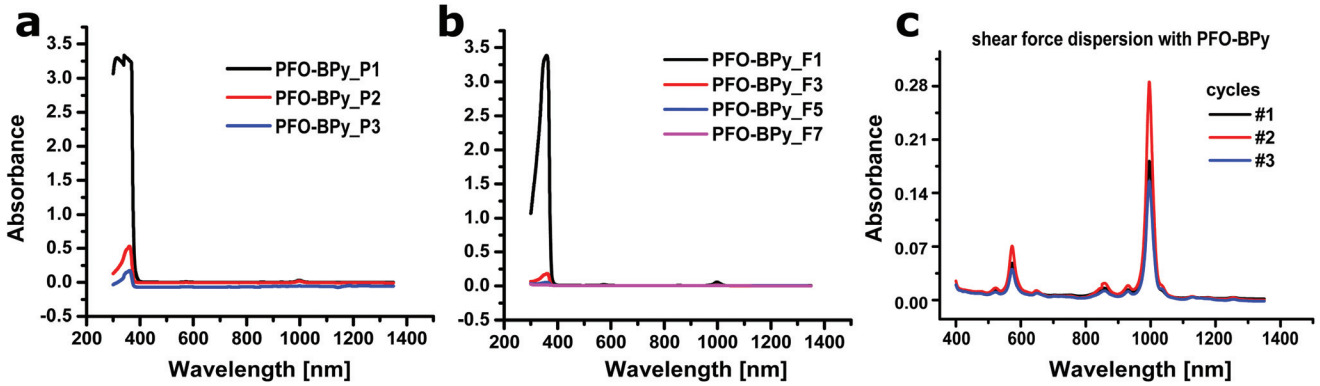

Fig. 2 Removal of PFO-polymer during the CPEP process. After large scale shear force mixing of (6,5)-SWCNTs with PFO-BPy in toluene the excess polymer is removed, which can be monitored by the PFO-BPy absorption peak at 300–400 nm. (a) Isopropyl alcohol addition decreases the colloidal stability of the SWCNTs and precipitates (P) them, while most of PFO-BPy stays in solution. Iteration of this progress decreases the concentration of the free PFO-BPy in the SWCNT sample (in toluene). (b) Stepwise filtration (F) process with 90 °C toluene removes the residue PFO-BPy of the SWCNT/NaCl pellet. (c) Dispersion of (6,5)-SWCNTs with recycled PFO-BPy shows that PFO-polymer can be reused.

SWCNTs (Fig. 2b), while SWCNTs adsorbed/agglomerated on and in between the filler. After drying and removing the NaCl, the purified (6,5)-SWCNT flakes were ready to be resuspended with any desired polymer. Addition of trifluoroacetic acid (TFA) to support PFO removal from SWCNTs decreased the nIR-fluorescence of redispersed (6,5)-SWCNTs and was therefore not used (see ESI Fig. S2†).

Combining the PFO-BPy supernatants furthermore enabled us to recycle and reuse the (expensive) PFO-BPy polymer for nanotube dispersion (see Fig. 2c).

The normalized absorption spectra of CPEP processed $(GT)_{10}$-(6,5)-SWCNTs, $(AT)_{15}$-(6,5)-SWCNTs and SDBS-(6,5)-SWCNTs are shown in Fig. 3a–c. The CPEP purified samples show as a major feature the S_{11} transition of the (6,5)-SWCNT but other chiralities have been substantially removed.

The S_{11} absorbance feature at around 890 nm (assigned to (6,4)-SWCNTs), 1040 nm (assigned to (7,5)-SWCNTs) and 1130 nm (mainly assigned to (7,6)/(8,4)-SWCNTs) are not any longer present in the highly enriched sample. Besides a reduced background in the S_{22} transition region, the phonon-sideband at around 850 nm becomes visible.

The SDBS sample shows a strong blue shift of the S_{11} and S_{22} transition, which could indicate a more effective debundling in the CPEP processed sample. Absorbance spectra were fitted (Fig. 3d–f) to quantify the ratio of SWCNT-chiralities. The S_{11} transitions showed that PFO-BPy dispersion yielded ~94% pure (6,5)-SWCNTs while resuspending in *e.g.* ssDNA did not change this enrichment significantly (87% for $(AT)_{15}$-(6,5) and 90% for $(GT)_{10}$-(6,5)-SWCNTs after CPEP), which is mainly attributed to differences in background and not the chirality composition itself. The yield of SWCNT dispersion could be further improved, by using a higher-power shear force mixer[36] instead of the customary homogenizer for shear force dispersion that was used here for CPEP.

We also evaluated the nanotube lengths after the CPEP of the two exemplaric ssDNA-SWCNTs and compared it with the one from the PFO-BPy-(6,5)-SWCNTs (see ESI Fig. S3†). The mean length from the PFO-BPy SWCNTs was ~1460 nm (SE 723 nm), which is slightly smaller than the length reported in literure.[36] Both ssDNA-(6,5)-SWCNT were in mean nearly half as long with 770 nm (SE 358 nm) for $(AT)_{15}$ and 757 nm (SE 347 nm) for $(GT)_{10}$. This results shows, that the resuspension of the purified (6,5)-SWCNTs obviously decreases the lateral mean size, while the absolute lengths is larger than the one, known from dispersing unpurified SWCNTs with ssDNA.[41]

The success of the purification procedure can be further visualized in SWCNT fluorescence spectra. Fig. 4a shows a 2D-fluorescence spectrum of ssDNA modified SWCNTs without further purification. It shows the emission of (6,5)-SWCNTs and other chiralities such as (6,4), (7,5) or (8,3). In contrast, the PFO-BPy modified SWCNTs (Fig. 4b) contain mainly (6,5)-SWCNTs as expected. The exchange to ssDNA and aqueous solution does not significantly (Fig. 4c and d) change the spectra. This result highlights how effective CPEP is to remove other chiralities and obtain monodisperse samples with a desired functionalization.

For biosensing application, it is of special interest whether CPEP processed and redispersed (6,5)-SWCNTs are still functional in terms of nIR-fluorescence responses to analytes. Fig. 5a shows a fluorescence spectrum of CPEP $(GT)_{10}$-(6,5)-SWCNTs and its increase after addition of dopamine [100 nM]. This type of functionalization is known to make SWCNTs responsive to the important neurotransmitter dopamine.[41,45] A single fluorescence peak of such sensors is essential for multiplexing approaches that use multiple SWCNT chiralities or other fluorophores. Therefore, monochiral samples could improve multiplexed sensing and imaging approaches for example to exploit differences in responsiveness by different chiralities.[50,62]

Another application that requires non-congested spectra is defect engineering.[13,63,64] These approaches lead new emission features and even to single-photon emitting SWCNTs and fun-

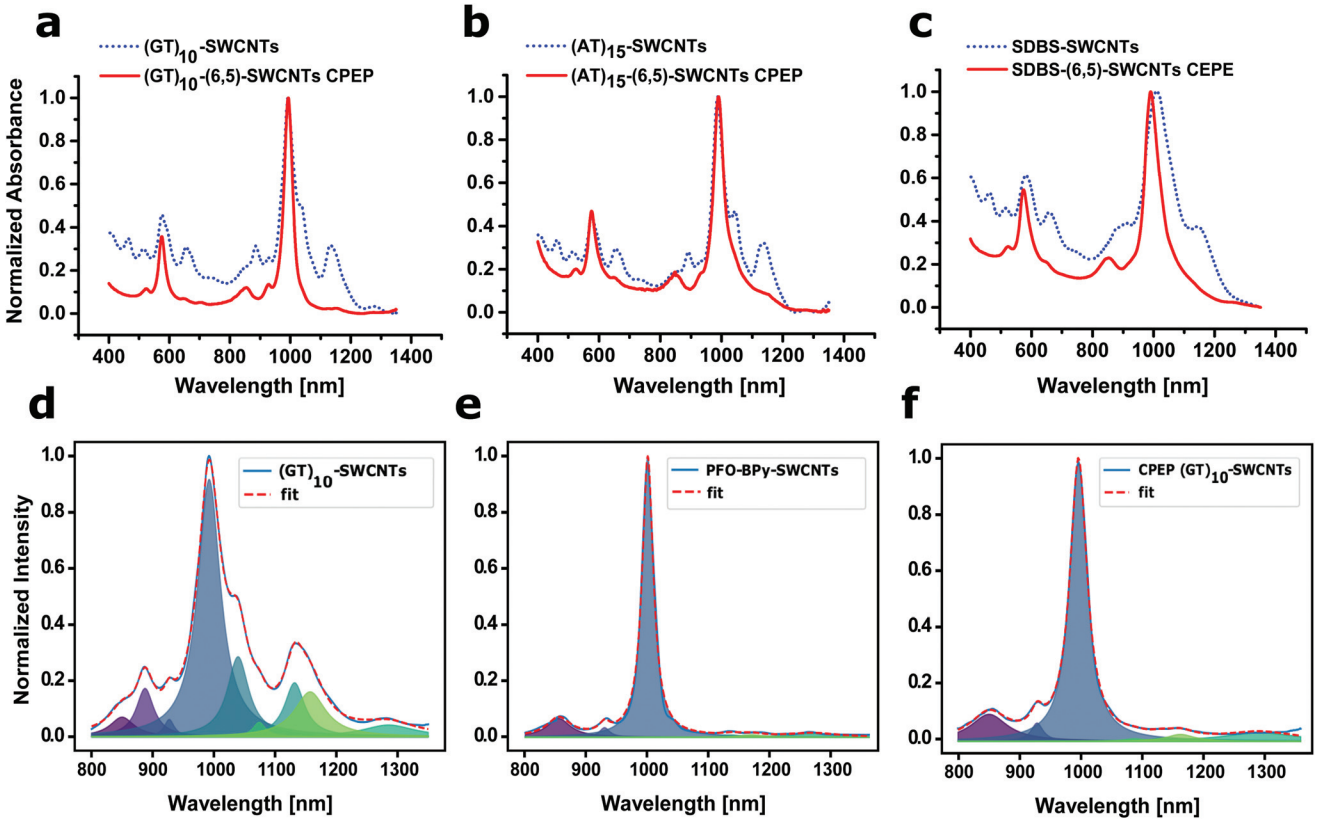

Fig. 3 Absorption spectra of corona phase exchange purified (6,5)-SWCNTs. Different functionalizations/coatings were used to resuspend the CPEP purified (6,5)-SWCNTs (red lines). Non-purified SWCNTs functionalized in the same way contain additional chiralities (blue dotted line). Two different ssDNA sequences (a) $(GT)_{10}$ and (b) $(AT)_{15}$ as well as (c) SDBS are shown as an example. The wavelengths of the absorption maxima are similar for ssDNA modified (6,5)-SWCNTs. CPEP purified SDBS SWCNTs showed a blue-shift, which indicates debundling compared to the non-purified sample. (d) Fitted absorption spectra of the raw SWCNT material, modified with $(GT)_{10}$-ssDNA. (e) Fitted absorption spectra of the raw SWCNT material, dispersed with PFO-BPy in toluene reveals a nearly monodisperse (6,5)-SWCNT sample. (f) Fitted absorption spectra of CPEP $(GT)_{10}$-SWCNTs displays again almost monodisperse (6,5)-SWCNTs.

damental insights into the mechanism rely on well-defined and unambiguous spectra. CPEP processed SWCNTs can be used to introduce defects as shown in Fig. 5b. The introduction of ($PhNO_2$) aryl sp^3-defects into the SWCNT surface causes a second, red-shifted fluorescence peak at ~1165 nm. Related studies with $PhNO_2$ defected SDBS-(6,5)-SWCNTs report E_{11}^{*} fluorescence maxima at ~1145 nm.[65]

Especially the tunable corona modification with different ssDNA sequences could help to improve SWCNT-based chemical sensing and imaging. Importantly, it expands the possibilities of non-covalent functionalization schemes to purified SWCNTs closer to covalent functionalization schemes.[66,67]

In addition to the modification of highly enriched (6,5)-SWCNTs with different ssDNA sequences and surfactants (see ESI Fig. S4†), it is possible to exchange the corona to biocompatible PEG-polymers (ESI Fig. S5†). Hereby, the purified SDBS- and PEG-(6,5)-SWCNTs showed a minor nIR-fluorescence peak at ~1120 nm, which cannot be monitored in the complimentary spectra from the raw nanotube material. Either other chiralities superimpose these features (see also ESI Fig. S6†), or they get enhanced due to the purification process. The spectral region of the minor peak could be assigned to oxygen induced defects to (6,5)-SWCNTs.[68]

Besides the specific dispersion of (6,5)-SWCNTs by PFO-BPy, other PFO-polymers are known to solubilize particular SWCNT chiralities.[35,69] Dispersing the crude SWCNT material with PFO in toluene, similar to the procedure using PFO-BPy, yielded highly enriched (7,5)-SWCNTs and a smaller fraction of (7,6)-SWCNTs (ESI Fig. S7†). Applying the CPEP, it was possible to remove PFO from the (7,5)-SWCNTs (see ESI Fig. S7a and b†) and further exchange the surface functionalization to different aqueous soluble surfactants or polymers (see ESI Fig. S8 and S9†). Therefore, the CPEP approach appears to be a general concept for PFO-polymer exchange, beyond the most used (6,5)-SWCNTs and PFO-BPy. Especially for SWCNT-based chemical imaging different specifically modified nanotube chiralities would be favorable to allow ratiometric sensing. By combining $(GT)_{10}$-(6,5)-SWCNTs and PEG-PL-(7,5)-SWCNTs (ESI Fig. S10†) it is in principle possible to create also a ratiometric dopamine sensor.

Besides the advantages of well-defined fluorescence features CPEP processed samples appear to be brighter compared

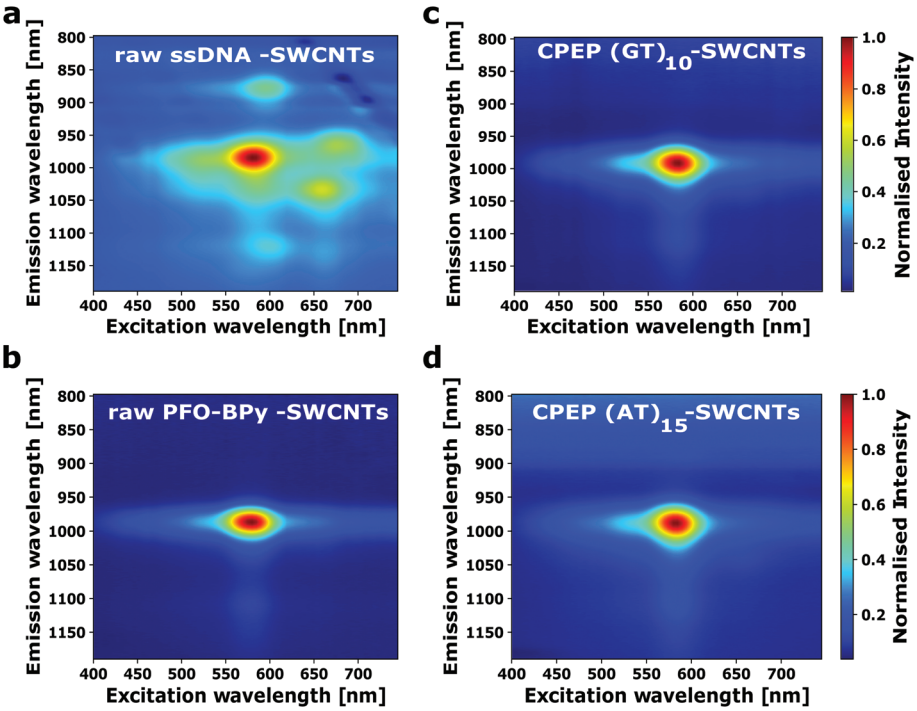

Fig. 4 2D excitation/emission spectra of CPEP-SWCNTs. (a) CoMoCAT SWCNT sample dispersed in $(GT)_{10}$-ssDNA. The major chirality is (6,5) but there are also (6,4), (7,5) and (8,3)-SWCNTs present. (b) PFO-BPy dispersed SWCNTs (in toluene) contain nearly exclusively (6,5)-SWCNTs. After removing PFO-BPy and resuspending the SWCNTs with ssDNA *via* the CPEP approach the same level of purity is achieved for (c) $(GT)_{10}$ or (d) $(AT)_{15}$-ssDNA functionalized SWCNTs in aqueous solution.

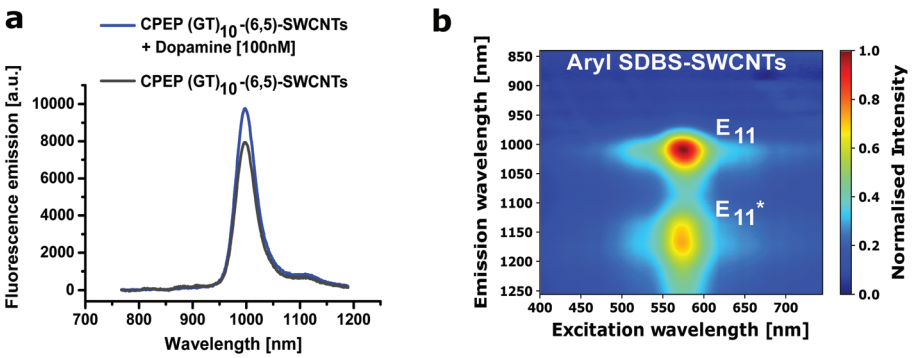

Fig. 5 Corona phase exchange purified SWCNTs for sensors and defect engineering. A major benefit of CPEP is the possibility to use any desired non-covalent surface modification, which is especially useful for sensors based on ssDNA-SWCNTs. (a) $(GT)_{10}$-(6,5)-SWCNTs increase their fluorescence in the presence of the neurotransmitter dopamine without interference from other chiralities. (b) Introducing sp^3 defects to SDBS-(6,5)-SWCNTs leads to a second well-defined red-shifted fluorescence peak that is not congested by other chiralities.

to similar non-purified samples with the same functionalization (ESI Fig. S11†). $(GT)_{10}$-(6,5)-SWCNTs display around 70% higher fluorescence intensities at the same concentration/absorption, which could be either explained by their increased length or the absence of quenching impurities.

The high monodispersity of CPEP processed SWCNTs is based on the specific dispersion of certain SWCNT chiralities by polyfluorene polymers.[37,38] This step relies also on the raw nanotube material and its ratio of semiconducting to metallic nanotubes and the containing chiralities.[70] Therefore, by choosing the appropriate SWCNT material and PFO-polymer for dispersion, CPEP can grant access to a brought range of enriched SWCNTs with desired surface modifications. This approach can be especially relevant for fundamental studies and applications of SWCNTs that require sophisticated surface chemistry beyond standard surfactants. Consequently, applications such as biosensors, imaging, drug delivery and defect engineering can profit from CPEP.

Conclusions

Chirality pure SWCNTs are necessary both for fundamental studies and biomedical applications. In this work we present a novel route to chirality enriched SWCNTs with tunable functionalization. It uses the selective dispersion of SWCNTs in PFO-polymers but removes/recycles them again and exchanges them to any non-covalent modification. These chirality enriched SWCNTs are functional and can be employed in applications for which the functionalization plays a crucial role and monodisperse spectra are essential such as single-emission fluorescence sensors and defect peak engineering.

Materials and methods

Purification protocol

Highly enriched (6,5)-SWCNTs were obtained based on the dispersion protocol from Graf *et al.*[36] 50 mg PFO-BPy (American Dye Source) were dissolved in 100 mL toluene by gently warming the solution. 25 mg chirality enriched (6,5)-SWCNTs (Sigma Aldrich, Product No. 773735) were added and placed for 20 h shear-force mixing (Homogenizer PT3100, Polytron) in a water bath, in order to keep the temperature during the surface modification process constantly at 20 °C. The following centrifugation step (15 min/20 500*g*/15 °C) yielded the highly enriched PFO-BPy-(6,5)-SWCNT stock solution. Two times 8 mL of the PFO-BPy-(6,5)-SWCNT solution were mixed with 2 ml isopropyl alcohol and centrifuged 15 + 5 min (20 500*g*/15 °C). This ratio of toluene to isopropyl alcohol led to a loss of the colloidal stability of the nanotubes, while the majority of the PFO-PBy stayed in solution. Lower ratios of isopropyl alcohol to toluene resulted in an incomplete precipitation of the SWCNTs, while a much higher ratio increased the amount of precipitated polymer. The (6,5)-SWCNT pellet was resuspended in 8 ml toluene and bath sonicated for 2 min. Afterwards, two more rounds of precipitation with isopropyl alcohol, centrifugation and resuspension were performed. The progress of PFO-BPy removal was followed by its UV-Vis absorption. The pellet was further transferred to a solvent resistant filter (2.2 NY, Ciro), which was equipped with 200 mg powdered NaCl crystals, which act as toluene-resistant but water-soluble filler/scaffold material. In the following washing step, the nanotube pellet was washed with 5 × 600 µl (90 °C) hot toluene, which removed the remaining PFO-BPy from the sample. The SWCNT loaded NaCl crystals were dried under vacuum and dialyzed for 24 h in a 1 kDa dialysis bag (Spectra/Por®) against ddH_2O. The resulting (6,5)-SWCNT flakes were transferred to a reaction tube, ready for further surface modification with a desired water-soluble surfactant. For ssDNA modification, 150 µl PBS and 125 µl (2 mg ml^{-1}) oligonucleotide solution were tip sonicated (30%, 45 min, Fisher ScientificTM Model 120 Sonic Dismembrator), followed by 10 min centrifugation at 10 000*g*. The same sonication conditions were used for SWCNT dispersion in 275 µl 0.2% SDBS aqueous solution. The residual PFO-BPy solution was evaporated and reused for SWCNT modification, while the undispersed SWCNT material was also recycled.[36] SWCNT dispersion with PFO was performed similarly using 1 mg ml^{-1} PFO in toluene.

UV-Vis-nIR absorption and nIR-fluorescence spectroscopy

UV-Vis-nIR absorbance spectra of the SWCNT conjugates were acquired with a JASCO V-670 device in a 10 mm path quartz cuvette. Fitting of absorption spectra was based on the approach by Pfohl *et al.*[71] In short, a background profile of the form $e^{-b\lambda}$ was fitted to the absorption spectra and subtracted. The normalized spectra were then fitted in Python to a function consisting in the sum of nine Lorentzians using a standard least squares fit, with the Trust Region Reflective algorithm.

1D and 2D nIR-fluorescence spectra were acquired with a Shamrock 193i spectrometer (Andor Technology Ltd, Belfast, Northern Ireland) connected to an IX53 microscope (Olympus, Tokyo, Japan). Excitation was performed with a Monochromator MSH150, equipped with a LSE341 light source (LOT-Quantum Design GmbH, Darmstadt, Germany). 200 µl of aqueous SWCNT conjugates were placed in a 96-well plate, while toluene-based samples were analyzed in a glass vial.

Conflicts of interest

There are no conflicts to declare.

Acknowledgements

This project was supported by the VW foundation. We thank Prof. Dr Andreas Janshoff and Prof. Dr Claudia Steinem as well as their groups for fruitful discussions and support.

Notes and references

1 A. Albanese, P. S. Tang and W. C. W. Chan, *Annu. Rev. Biomed. Eng.*, 2012, **14**, 1–16.
2 M. L. Personick and C. A. Mirkin, *J. Am. Chem. Soc.*, 2013, **135**, 18238–18247.
3 J. Li and G. P. Pandey, *Annu. Rev. Phys. Chem.*, 2015, **66**, 331–356.
4 V. Z. Zamolo, E. Vazquez and M. Prato, *Top. Curr. Chem.*, 2013, **286**, 1–72.
5 M. S. Arnold, J. L. Blackburn, J. J. Crochet, S. K. Doorn, J. G. Duque, A. Mohite and H. Telg, *Phys. Chem. Chem. Phys.*, 2013, **4**, 1166–1169.
6 A. R. Amori, Z. Hou and T. D. Krauss, *Annu. Rev. Phys. Chem.*, 2018, **69**, 81–100.
7 S. M. Bachilo, M. S. Strano, C. Kittrell, R. H. Hauge, R. E. Smalley and R. B. Weisman, *Science*, 2002, **298**, 2361–2367.

8 S. Nanot, E. H. Hároz, J. H. Kim, R. H. Hauge and J. Kono, *Adv. Mater.*, 2012, **24**, 4977–4994.
9 M. J. O. Connell, S. M. Bachilo, C. B. Huffman, K. L. Rialon, P. J. Boul and W. H. Noon, *Science*, 2002, **297**, 593–597.
10 G. Hong, S. Diao, A. L. Antaris and H. Dai, *Chem. Rev.*, 2015, **115**, 10816–10906.
11 S. Kruss, A. J. Hilmer, J. Zhang, N. F. Reuel, B. Mu and M. S. Strano, *Adv. Drug Delivery Rev.*, 2013, **65**, 1933–1950.
12 C. Farrera, F. Torres Andón and N. Feliu, *ACS Nano*, 2017, **11**, 10637–10643.
13 X. He, H. Htoon, S. K. Doorn, W. H. P. Pernice, F. Pyatkov, R. Krupke, A. Jeantet, Y. Chassagneux and C. Voisin, *Nat. Mater.*, 2018, **17**, 663–670.
14 E. Polo and S. Kruss, *Anal. Bioanal. Chem.*, 2016, **408**, 2727–2741.
15 J. Prasek, J. Drbohlavova, J. Chomoucka, J. Hubalek, O. Jasek, V. Adam and R. Kizek, *J. Mater. Chem.*, 2011, **21**, 15872–15884.
16 J.-Q. Wang, F. Ding, D. Luo, D. Zhang, X. Wang, J. Yang, X. Bai, F. Peng, Z. Xu, J. Wei, Y. Li, M. Li, R. Li, F. Yang, X. Li, Y. Li and Z. Xu, *Nature*, 2014, **510**, 522–524.
17 H. An, A. Kumamoto, H. Takezaki, S. Ohyama, Y. Qian, T. Inoue, Y. Ikuhara, S. Chiashi, R. Xiang and S. Maruyama, *Nanoscale*, 2016, **8**, 14523–14529.
18 A. S. R. Bati, L. Yu and M. Batmunkh, *Nanoscale*, 2018, **10**, 22087–22139.
19 D. Janas, *Mater. Chem. Front.*, 2017, **2**, 36–63.
20 M. C. Hersam, *Nat. Nanotechnol.*, 2008, **3**, 387–394.
21 J. Cui, D. Yang, X. Zeng, N. Zhou and H. Liu, *Nanotechnology*, 2017, **28**, 452001.
22 M. Zheng, *Top. Curr. Chem.*, 2017, **375**, 1–36.
23 M. S. Arnold, A. A. Green, J. F. Hulvat, S. I. Stupp and M. C. Hersam, *Nat. Nanotechnol.*, 2006, **1**, 60–65.
24 S. Ghosh, S. M. Bachilo and R. B. Weisman, *Nat. Nanotechnol.*, 2010, **5**, 443–450.
25 J. A. Fagan, C. Y. Khripin, C. A. Silvera Batista, J. R. Simpson, E. H. Hároz, A. R. Hight Walker and M. Zheng, *Adv. Mater.*, 2014, **26**, 2800–2804.
26 C. Y. Khripin, J. A. Fagan and M. Zheng, *J. Am. Chem. Soc.*, 2013, **135**, 6822–6825.
27 S. Reich, H. Li, O. Garrity, B. S. Flavel and G. Gordeev, *ACS Nano*, 2019, **13**, 2567–2578.
28 H. Liu, D. Nishide, T. Tanaka and H. Kataura, *Nat. Commun.*, 2011, **2**, 1–8.
29 H. Liu, T. Tanaka, Y. Urabe and H. Kataura, *Nano Lett.*, 2013, **13**, 1996–2003.
30 B. S. Flavel, M. M. Kappes, R. Krupke and F. Hennrich, *ACS Nano*, 2013, **7**, 3557–3564.
31 K. Tvrdy, R. M. Jain, R. Han, A. J. Hilmer, T. P. Mcnicholas and M. S. Strano, *ACS Nano*, 2013, **2**, 1779–1789.
32 X. Tu, S. Manohar, A. Jagota and M. Zheng, *Nature*, 2009, **460**, 250–253.
33 M. Zheng, A. Jagota, M. S. Strano, A. P. Santos, P. Barone, S. G. Chou, B. A. Diner, M. S. Dresselhaus, R. S. Mclean, G. B. Onoa, G. G. Samsonidze and E. D. Semke, *Science*, 2003, **302**, 1545–1549.
34 M. Zheng, A. Jagota, E. D. Semke, B. A. Diner, R. S. McLean, S. R. Lustig, R. E. Richardson and N. G. Tassi, *Nat. Mater.*, 2003, **2**, 338–342.
35 N. Ide and N. Yasuro, *Chem. Lett.*, 2011, 239–241.
36 A. Graf, Y. Zakharko, S. P. Schießl, C. Backes, M. Pfohl, B. S. Flavel and J. Zaumseil, *Carbon*, 2016, **105**, 593–599.
37 F. Hennrich, S. Lebedkin and M. M. Kappes, *J. Phys. Chem. C*, 2009, **113**, 14628–14632.
38 A. Nish, J. Y. Hwang, J. Doig and R. J. Nicholas, *Nat. Nanotechnol.*, 2007, **2**, 640–646.
39 J. Pan, F. Li and J. H. Choi, *J. Mater. Chem. B*, 2017, **5**, 6511–6522.
40 S. Kruss, M. P. Landry, E. Vander Ende, B. M. A. Lima, N. F. Reuel, J. Zhang, J. Nelson, B. Mu, A. Hilmer and M. Strano, *J. Am. Chem. Soc.*, 2014, **136**, 713–724.
41 R. Nißler, F. A. Mann, P. Chaturvedi, J. Horlebein, D. Meyer, L. Vukovic and S. Kruss, *J. Phys. Chem. C*, 2019, **123**, 4837–4847.
42 D. Meyer, A. Hagemann and S. Kruss, *ACS Nano*, 2017, **11**, 4017–4027.
43 G. Bisker, J. Ahn, S. Kruss, Z. W. Ulissi, D. P. Salem and M. S. Strano, *J. Phys. Chem. C*, 2015, **119**, 13876–13886.
44 S. Kruss, D. P. Salem, L. Vuković, B. Lima, E. Vander Ende, E. S. Boyden and M. S. Strano, *Proc. Natl. Acad. Sci. U. S. A.*, 2017, **114**, 1789–1794.
45 F. A. Mann, N. Herrmann, D. Meyer and S. Kruss, *Sensors*, 2017, **17**, 1521.
46 E. Polo, T. Nitka, E. Neubert, L. Erpenbeck, L. Vuković and S. Kruss, *ACS Appl. Mater. Interfaces*, 2018, **10**, 17693–17703.
47 A. J. Gillen, J. Kupis-rozmysłowicz, C. Gigli, N. Schuergers and A. A. Boghossian, *J. Phys. Chem. Lett.*, 2018, **9**, 4336–4343.
48 A. F. Mann, J. Horlebein, N. F. Meyer, F. Thomas and S. Kruss, *Chem. – Eur. J.*, 2018, **24**, 12241–12245.
49 N. E. Kallmyer, J. Musielewicz, J. Sutter and N. F. Reuel, *Anal. Chem.*, 2018, **90**, 5209–5216.
50 G. Bisker, J. Dong, H. D. Park, N. M. Iverson, J. Ahn, J. T. Nelson, M. P. Landry, S. Kruss and M. S. Strano, *Nat. Commun.*, 2016, **7**, 1–14.
51 R. M. Williams, C. Lee and D. A. Heller, *ACS Sens.*, 2018, **3**, 1838–1845.
52 F. A. Mann, Z. Lv, J. Grosshans, F. Opazo and S. Kruss, *Angew. Chem., Int. Ed.*, 2019, DOI: 10.1002/anie.201904167.
53 J. K. Streit, A. Fagan and M. Zheng, *Anal. Chem.*, 2017, **89**, 10496–10503.
54 J. P. Giraldo, M. P. Landry, S. Y. Kwak, R. M. Jain, M. H. Wong, N. M. Iverson, M. Ben-Naim and M. S. Strano, *Small*, 2015, **11**, 3973–3984.
55 K. Welsher, Z. Liu, S. P. Sherlock, J. T. Robinson, Z. Chen, D. Daranciang and H. Dai, *Nat. Nanotechnol.*, 2009, **4**, 773–780.
56 X. Wu, M. Kim, H. Kwon and Y. H. Wang, *Angew. Chem., Int. Ed.*, 2018, **57**, 648–653.
57 C. Kanimozhi, G. J. Brady, M. J. Shea, P. Huang, Y. Joo, M. S. Arnold and P. Gopalan, *ACS Appl. Mater. Interfaces*, 2017, **9**, 40734–40742.

58 Y. Joo, G. J. Brady, M. J. Shea, M. B. Oviedo, C. Kanimozhi, S. K. Schmitt, B. M. Wong, M. S. Arnold and P. Gopalan, *ACS Nano*, 2015, **9**, 10203–10213.
59 S. Liang, Y. Zhao and A. Adronov, *J. Am. Chem. Soc.*, 2014, **136**, 970–977.
60 T. Lei, X. Chen, G. Pitner, H. S. P. Wong and Z. Bao, *J. Am. Chem. Soc.*, 2016, **138**, 802–805.
61 I. Pochorovski, H. Wang, J. I. Feldblyum, X. Zhang, A. L. Antaris and Z. Bao, *J. Am. Chem. Soc.*, 2015, **137**, 4328–4331.
62 E. Polo and S. Kruss, *J. Phys. Chem. C*, 2016, **120**, 3061–3070.
63 H. Kwon, L. R. Powell, G. C. Schatz, B. Meany, N. Valley, Y. Piao and Y. Wang, *Nat. Chem.*, 2013, **5**, 840–845.
64 X. He, N. F. Hartmann, X. Ma, Y. Kim, R. Ihly, J. L. Blackburn, W. Gao, J. Kono, Y. Yomogida, A. Hirano, T. Tanaka, H. Kataura, H. Htoon and S. K. Doorn, *Nat. Photonics*, 2017, **11**, 577–582.
65 T. Shiraki, S. Uchimura, T. Shiraishi, H. Onitsuka and N. Nakashima, *Chem. Commun.*, 2017, **53**, 12544–12547.
66 M. Prato, K. Kostarelos and A. Bianco, *Acc. Chem. Res.*, 2008, **41**, 275–294.
67 D. Tasis, N. Tagmatarchis, A. Bianco and M. Prato, *Chem. Rev.*, 2006, **106**, 1105–1136.
68 S. Ghosh, S. M. Bachilo, R. A. Simonette, K. M. Beckingham and R. B. Weisman, *Science*, 2010, **330**, 1656–1659.
69 F. Jakubka, S. B. Grimm, Y. Zakharko, F. Gannott and J. Zaumseil, *ACS Nano*, 2014, 8477–8486.
70 S. Liang, H. Li, B. S. Flavel and A. Adronov, *Chem. – Eur. J.*, 2018, **24**, 9799–9806.
71 M. Pfohl, D. D. Tune, A. Graf, J. Zaumseil, R. Krupke and B. S. Flavel, *ACS Omega*, 2017, **2**, 1163–1171.